UDC 534.232

PREPROCESSING AND ENHANCING IMAGE QUALITY OF TOMOGRAPHY OPTOACOUSTIC RECONSTRUCTION

A. G. Rudnitskii, M. A. Rudnytska, L. V. Tkachenko[†]

Institute of Hydromechanics of NAS of Ukraine Zhelyabov Str., 8/4, 03057, Kyiv, Ukraine †E-mail: lusia.tkch@gmail.com

Received 11.09.2017

The photoacoustic method offers excellent optical contrast combined with deep ultrasonic penetration and resolution for structural and functional medical imaging. In this work, we focus on designing the 3D filter for efficient and comprehensive suppression of different kinds of noises that could coexist in photoacoustic signals. We consider spatial filters with only one parameter to tune: the window size. The Median-Modified Wiener Filter (MMWF) and Iterative Truncated Arithmetic Mean Filter (ITM) were compared with well-established denoising techniques (Mean, Median, and Wiener Filters) to suggest the best approach to practical use. Their performance was tested using Shepp-Logan phantom of size $256 \times 256 \times 256$ voxels. In addition to the visual quality, we considered the Signal-to-Noise Ratio (SNR), Mean Square Error (MSE), Peak Signal-to-Noise Ratio (PSNR), and Structural Similarity Index (SSIM). Performance of the proposed filters was also assessed in terms of processing time. Simulation results reveal that the ITM and MMWF filters outperform the existing state of art filters by providing better visual quality along with PSNR, SSIM, and MSE values for the Shepp-Logan phantom corrupted by the Gaussian or impulse noise and the mix of these noises.

KEY WORDS: denoising, image processing, noise reduction filter, spatial filtering, photoacoustic imaging, fuzzy sets

1. INTRODUCTION

In the last decade, photoacoustic (PA) imaging is one of the fastest growing biomedical imaging modality. This method has multiple already implemented and envisioned applications in biomedical research and clinical practice (diagnostic applications in cancer research, brain imaging, drug development and treatment monitoring). The power of the technique is that it draws upon the advantages of high optical absorption contrast and deep ultrasonic penetration. But, there are multiple frontiers still open for many challenges related to removal of image artifacts, multi-spectral data processing, image quantification, reconstruction strategies and real-time operations. One of these problems is denoising of PA signals.

It is well known, that bandwidth of PA signals can be quite wide (several tens of MHz). There are two reasons for this. The first one is that it depends on the duration of the light pulse. The second reason is that frequency spectrum of the PA signals depend on the size of the target [1]. In addition, PA signals are very sensitive to noise generated by peripheral equipment (power supply, stepping motor of semiconductor laser and so on). Due to these reasons, the recorded PA signal is modified from its original pressure profile. That is why in real life we meet with situation when the spectrum of the noise overlaps the bandwidth of the PA signal. This effect leads to a degradation of components of PA signal. So, without signal preprocessing, the reconstruction images might suffer from low signal-to-noise ratio and low resolution.

Since denoising is at the very beginning of the preprocessing operations, it has a great impact on the results of down-stream steps. The main advantage of a good denoising is that it can prevents the overestimation of the image background and helps extracting faint, yet significant, features, while prevent the formation of misleading features [2].

There are several ways to reduce the noise level from the raw data: signal averaging, "moving averaging" or frequency filtering. However, signal averaging time is limited by physiological changes in the tissue, tissue movement due to breaths or heartbeats, muscle movements and shifts of another nature. Thus, the averaged raw data can still contain significant noise. "Moving averaging" works like a low-pass filter: it is suitable for suppressing high frequency noises when the signal itself contains primarily low frequency components. Frequency filtering can substantially suppress the noise level if the noise spectrum has limited overlap with the real PA pressure profile spectrum. However, the "moving averaging" method can smear out sharp changes in the original signal, and the frequency filtering method can potentially discard useful frequency components overlapped with noise. So, the shape of PA signals and kinds of noise is too complicated for these methods of filtering and often the results are unsatisfied. Therefore, it has great practical significance to find a new filter method with better filtering precision and noise suppression.

It is important to notice that most previous methods of noise reduction in PA signals are based on a quasi-three-dimensional approach, when sensor data on the surface are cleaned consecutively from one moment of time to next moment. Then is formed a three-dimensional image data composed of pure slices. This approach transforms three-dimensional spatial-temporal problem into a set of two dimensional spatial problems. But this method destroys the close relationship between slices in time domain. The residual noise and denoising artifacts differ from frame to frame causing in this way an unpleasant "flickering" effect. Therefore, the results of reconstruction, based on this approach, are unsatisfactory. Furthermore, in PA imaging, the problem of reconstruction is always three-dimensional. This is due to the nature of the optoacoustic effect, when the recovery requires collecting information from the entire volume. This means that the more reasonable and natural method is 3-dimensional filtering when the object of filtration is the original 3D image.

Due to the above reasons, the objective of the present study was to design of simple 3D filter for effective and comprehensive suppression of different kind of noises that could coexist in PA signals.

2. IN SILICO EXPERIMENT

To predict the effects of different kinds of noise to real data different kinds of artificial random noise was added to simulated image. The resulting noisy images were used as input for the different filters.

For evaluating of performance of developed algorithms we used 3D Shepp-Logan head phantom — a test image used widely by researchers in tomography. This phantom consists of a number of ellipses of varying sizes and densities. The Shepp-Logan phantom was selected as a reference due to its simplicity, yet appositeness in representing prominent anatomical features of the human head, as well as its omnipresence among the image processing community.

Datasets of corrupted by noise images were created with 10 dB peak signal-to-noise-ratio (PSNR) for Gaussian noise, "salt&pepper noise", mixture of Gaussian and Alpha-stable noise, mixture of Gaussian and Speckle noise.

These noisy images were used to predict which noise reduction methods are likely to be fruitful, as well as to provide a comparison of the effects of noise on the different filtering algorithms.

3. NOISE

It should be emphasized that noise within a real digital image does not arise from a single source. Every element in imaging chain contributes to noise.

In the real practice, the types and mixtures of noises present in the images are not known a priori. That's why we used rather general model for a mixed-type noise which contains the additive and exclusive noise:

$$g(d_1, \dots, d_n) = \begin{cases} f(d_1, \dots, d_n) + n(d_1, \dots, d_n) & \text{with probability } p, \\ e(d_1, \dots, d_n) & \text{with probability } 1 - p, \end{cases}$$

where $g(d_1, \ldots, d_n)$ is the corrupted image, $f(d_1, \ldots, d_n)$ is the original signal (image), $n(d_1, \ldots, d_n)$ is the additive noise (it can be short- or long-tailed noise, such as Gaussian or Laplacian noise) and $e(d_1, \ldots, d_n)$ denote exclusive noise. The exclusive noise could be impulsive noise, such as pepper&salt noise. The occurrence probability of the two types of noise is controlled by $p \in [0, 1]$. The exclusive noise occurs if p is smaller than 1.

For additive noise we used Alpha stable noise.

Alpha stable noise, also called Lévy noise, was put forward by Lévy when he studied the Generalized Central Limit Theorem [3,4]. Alpha stable distribution is widely used to analyze and model signals for many reasons: there exist many non-Gaussian signals with an impulsive nature and heavy tail in real life, including underwater signals, atmospheric environment signals, telephone line noise and some mobile communication signals and so on.

There is no closed-form expression for the probability density of alpha stable noise, but

it can be described by its characteristic function, which can be expressed as follows:

$$\phi(t) = \exp\left(it\mu - \gamma^{\alpha}|t|^{\alpha}[1 - i\beta\operatorname{sign}(t)\omega(t,\alpha)]'\right),$$

$$\omega(t,\alpha) = \begin{cases} \operatorname{tg}(\pi\alpha), & \alpha \neq 1, \\ \frac{2}{\pi}\ln|t|, & \alpha = 1, \end{cases}$$

where α is the characteristic exponent and the most important parameter characterizing alpha stable noise $(0 < \alpha \le 2)$. The smaller the value of α is, the more severe the heavy tail of the distribution is, as is its impulsive nature.

When $\alpha = 2$, the alpha stable distribution becomes a Gaussian distribution with mean μ and variance $\sigma^2 = 2\gamma^2$. In the cases of $\alpha = 1$, $\beta = 0$ and $\alpha = 1/2$, $\beta = 1$, the alpha stable distribution becomes a Cauchy distribution and a Lévy distribution respectively.

Next type of noise which is very important in PA is speckle noise [5]. It is a "granular" noise that commonly observed in almost all coherent imaging systems such as laser, acoustics and SAR (Synthetic Aperture Radar) imagery. The source of this noise is attributed to random interference between the coherent returns. In this case, the waves emitted by active sensors travel in phase and interact minimally on their way to the target area. After interaction with the target area, these waves are no longer in phase because of scattering. Once out of phase, waves can interact to produce light and dark pixels known as speckle noise. Images with speckle noise will results in reducing the contrast of image and difficult to perform image processing operations like edge detection or segmentation. It has been experimentally verified in several works that over homogeneous areas, the standard deviation of the signal is proportional to its mean. This fact suggests the use of the multiplicative model for the speckle noise.

We assumed that offered models may be most adequate to real medicine practice.

4. DESIGN OF FILTERS

Most denoising methods require that some of its parameters be set manually to optimize their performance. These filters can give very high performance but very often they are impractical in real medicine condition. That's why we decided to use simplest spatial filters which have only one control parameter — window size. This parameter is related to the minimum size of the feature to be considered in the image analysis and is intuitive clear in real practice.

The first two spatial filters that we considered are the mean and median filters. The mean filter is a simplest linear filter while the median is a simplest nonlinear filter.

The mean filter is optimal in suppressing of additive Gaussian noise. On this base emerge rich class of the linear finite impulse response (FIR) filters which are effective in attenuating the additive Gaussian noise but not the long-tailed noise. Moreover mean filter blurs image structures.

On the contrary, the median filter has the advantages in suppressing the long-tailed noise. This filter is optimal for the removal of impulse noise on images and does not blur edges. Its disadvantages, mainly the inflexibility in the filter structure, the destruction of fine image

details, and its relatively poor performance in attenuating additive Gaussian noise and other short-tailed noise.

More advanced linear technique for spatial filtering is the Wiener filter (Minimum mean-square error (MMSE) filter), which exhibits varying behavior based on local image statistics. Wiener filter is applied to a signal adaptively, tailoring itself to the local signal variance. This filter performs less smoothing where the variance is large, while where the variance is small, it performs more smoothing. It works best with Gaussian or uniform noise and for n-dimensional hypercube is defined as follows:

$$b_w(d_1, \dots, d_n) = \mu + \frac{\sigma^2 - \nu^2}{\sigma^2} [a(d_1, \dots, d_n) - \mu],$$

where d_1, \ldots, d_n is the location of a discrete point in an n-dimensional hypercube;

$$\mu = \frac{1}{\prod_{i=1,\dots,n} D_i} \sum_{d_1,\dots,d_n \in \eta} a(d_1,\dots,d_n)$$

is local (i.e., considered in the sliding window) mean, D_i - the length of the i-th dimension of the hypercube;

$$\sigma^{2} = \frac{1}{\prod_{i=1,\dots,n} D_{i}} \sum_{d_{1},\dots,d_{n} \in \eta} [a(d_{1},\dots,d_{n}) - \mu]^{2}$$

is variance around each pixel in *n*-dimensional signal; $a(d_1, \ldots, d_n)$ is a notation to identify each pixel contained in the area η of the *n*-dimensional signal.

By operating in this manner, the MMSE filter preserves image details while removes noise and often produces better results than standard non adaptive linear filtering.

To merge the complementary qualities and abilities of median filter and the Wiener filter, reciprocally nullifying the respective defects was suggested nonlinear adaptive spatial filter (Median-Modified Wiener filter MMWF) [6]:

$$b_{mmwf}(d_1,\ldots,d_n) = \tilde{\mu} + \frac{\tilde{\sigma}^2 - \tilde{\nu}^2}{\tilde{\sigma}^2} [a(d_1,\ldots,d_n) - \tilde{\mu}],$$

where $\tilde{\mu} = \text{Median}[a(d_1, \dots, d_n)]$ is local (i.e., considered in the sliding window) median;

$$\tilde{\sigma}^2 = \frac{1}{\prod_{i=1,\dots,n} D_i} \sum_{d_1,\dots,d_n \in \eta} [a(d_1,\dots,d_n) - \tilde{\mu}]^2$$

is variance around each pixel in n-dimensional signal average squared deviation from the median $\tilde{\mu}$.

This modification in the original Wiener filter formula has very significant consequences which are caused by the introduction in an adaptive contest of the median operator.

In particular, this filter facilitates removing spike noise from the signal background (typical of the median filter) while preserving unaltered edges. Last property partially provided by the Wiener filter that preserves edges but unfortunately modifying their morphology. The median operator is much less affected by these outlier values in the distribution of the local variances, thus provides a more robust estimation of the noise variance [6].

The merits of the mean and median filters lead also to another branch of filters which make compromises between these two filters. The iterative truncated arithmetic mean (ITM) filter has been recently proposed [7]. It iteratively truncates the extreme values of samples in the filter window to a dynamic threshold. This threshold guarantees that the filter output converges to the median of the input samples. A proper stop criterion enables the ITM filter owning merits of both the arithmetic mean and the order-statistical median operations.

5. METHODS OF FILTERS TESTING

There were chosen four measures of noise reduction quality: normalized mean square error (MSE), signal to noise ratio (SNR), peak signal to noise ratio (PSNR) and Structural Similarity Index (SSIM).

This metrics are expressed (in dB) as

$$PSNR = 20 \log_{10} \left(\frac{MAX_I}{\sqrt{MSE}} \right),$$

$$CNR = 101 \qquad \left(\frac{P_{\text{signal}}}{\sqrt{MSE}} \right)$$

$$SNR = 10 \log_{10} \left(\frac{P_{\text{signal}}}{P_{\text{noise}}} \right),$$

MSE =
$$\frac{1}{mn} \sum_{i=0}^{m-1} \sum_{j=0}^{n-1} [I(i,j) - K(i,j)]^2$$
.

Here, MAX_I is the maximum possible pixel value of the image (when the pixels are represented using 8 bits per sample, this is 255); I(i,j) is noise-free $m \times n$ gray scale image; K(i,j) is its noisy approximation; P is average power.

These methods directly measure the pixel-by-pixel differences between the images. They are attractive metrics for the loss of image quality due to its simplicity and mathematical convenience. But they are not well matched to perceive visual quality.

An alternative framework, for quality assessment based on the degradation of structural information is Structural Similarity index [8]. SSIM is designed to improve on traditional methods such as PSNR and MSE, which have proven to be inconsistent with human visual perception. SSIM assesses the visual impact of three characteristics of an image: luminance l(x, y), contrast c(x, y) and structure s(x, y). The overall index is a multiplicative combination of the three terms:

$$SSIM(x,y) = [l(x,y)]^{\alpha} [c(x,y)]^{\beta} [s(x,y)]^{\gamma},$$

where

$$l(x,y) = \frac{2\mu_x \mu_x + c_1}{\mu_x^2 + \mu_y^2 + c_1}; \qquad c(x,y) = \frac{2\sigma_x \sigma_y + c_2}{\sigma_x^2 + \sigma_y^2 + c_2}; \qquad s(x,y) = \frac{\sigma_{xy} + c_3}{\sigma_x \sigma_y + c_3};$$

 μ_x , μ_y , σ_x , σ_y , and σ_{xy} are the local means, standard deviations, and cross-covariance for images. If $\alpha = \beta = \gamma = 1$ (the default for exponents), and $c_3 = c_2/2$ (default selection of c_3) the index simplifies to:

SSIM
$$(x, y) = \frac{(2\mu_x \mu_y + c_1)(2\sigma_{xy} + c_2)}{(\mu_x^2 + \mu_y^2 + c_1)(\sigma_x^2 + \sigma_y^2 + c_2)},$$

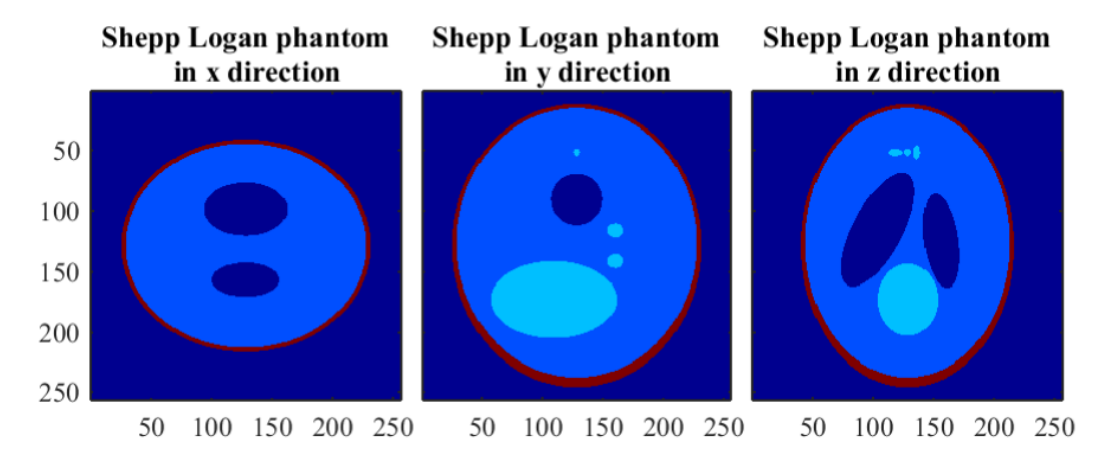


Fig. 1. Central slices of the 3D Shepp-Logan phantom

 $c_1 = (k_1 L)^2$ and $c_2 = (k_2 L)^2$ are two variables to stabilize the division with weak denominator; L is a dynamic range of the pixel-values (typically, this is $2^{\text{bits/pixel}} - 1$); $k_1 = 0.01$ and $k_2 = 0.03$. The resultant SSIM index is a decimal value between -1 and 1, and value 1 is only reachable in the case of two identical sets of data.

Firstly, for evaluating of performance of developed algorithms we used 3D Shepp-Logan head phantom being a test image used widely by researchers in tomography. Fig. 1 shows central sections of this 3D image.

Images corrupted by noise were used to predict which methods of noise reduction were likely to be fruitful, as well as to provide a comparison of the effects of noise on the different filtering algorithms. Datasets were created with 10 dB peak signal-to-noise-ratio (PSNR) for Gaussian noise and for mixture of Gaussian and Alpha-stable noise. There were applied 5 designed 3D filters: mean filter, median filter, spatial Wiener filter, modified median filter and Iterative Truncated Arithmetic Mean Filter. In all cases for all filters were used 3-voxels windows (kernels). Shepp-Logan phantom was $256 \times 256 \times 256$ size (in voxels). For the first three filters filtering was used twice for the same image and for Iterative Truncated Arithmetic Mean Filter we used 3 iterations. Examples of images generated from these noisy datasets are included below Fig. 2a shows results of filtering 3D images corrupted by Gaussian noise with PSNR=10 dB, and Fig. 2b shows results of filtering for mix of Gaussian and impulse noise with PSNR=10 dB.

After applying of these four denoising methods the closest reconstruction to the "ground truth" image (Fig. 1) in the Shepp-Logan case was obtained using MMWF and ITM technique. This is confirmed in the plots (Fig. 3), which depict cross-sections through a central region of the phantom. It can be observed that for these filters the borders of the analyzed region are well preserved, and only small deviations from the ground truth are present (Figs. 2 and 3).

Tab. 1 summarizes the comparison between the performance of different kinds of filters for one of more practical mix of noises, namely, the sum of Gaussian and alpha-stable noise (PSNR = 15 dB). There were conducted 20 numerical experiments for every kinds of noise for every filter and then averaged metrics were calculated. Evidently, the best result gives MMWF filter, however at a steep computational cost.

Fig. 4 demonstrates the performance of the proposed filters for other combinations of

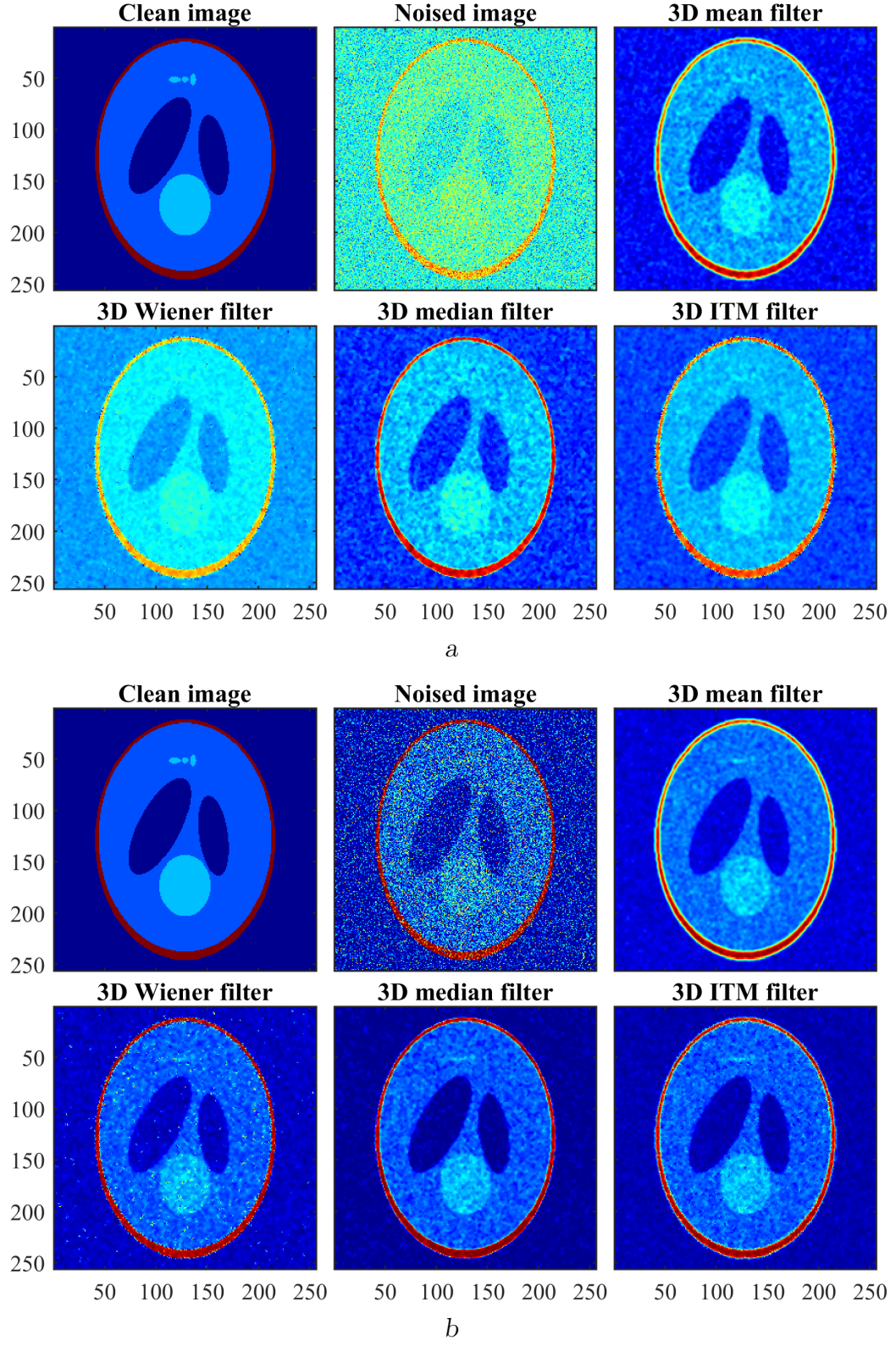


Fig. 2. Simulation results for central transverse slice of the Shepp-Logan phantom corrupted with noise (PSNR=10 dB):

a — Gaussian noise, b — mix of Gaussian and impulse noise

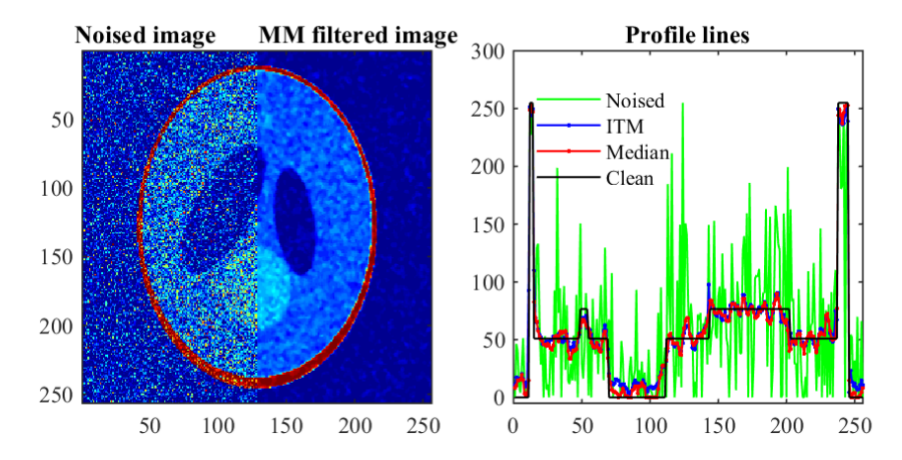


Fig. 3. Central transverse slice in a Shepp-Logan phantom with mix of Gausian and Alpha stable noise (right part) and after MMWF filtering (left part) along with profile lines of the central slices over a central region. The noise-free data profile is shown in black, noisy profile in green, ITM profile in light blue dot line, median profile in red dot line

Filter	MSE	SNR	PSNR	SSIM	Time (s)
Noise	2057.5 ± 16	50.96 ± 0.03	15.00 ± 0.03	0.09	
Mean	680.2 ± 3	55.77 ± 0.02	19.80 ± 0.02	0.11	7
Wiener	482.28 ± 7	57.26 ± 0.06	21.30 ± 0.06	0.13	8
MMWF	113.55 ± 2	63.54 ± 0.07	27.58 ± 0.07	0.16	485
ITM	271.98 ± 4	59.75 ± 0.09	23.79 ± 0.09	0.14	53

Tab. 1. Mix of Gaussian and Alpha stable noise

filters and noises. All measures were normalized to be comparable.

We see that almost always the MMWF and ITM filters scored first or second in each single denoising category (Gaussian or salt&pepper noise) and are the best filters for denoising of mixture of different kinds of noise. Unfortunately ultimate decision for global evaluation of denoising quality is not simple problem because of a lot of amount of data.

It is especially clear if take into account that the fulfillment time may be very important to evaluate of the performance of the different algorithms. An algorithm can lose its interest if its runtime delays the normal workflow of a service. Hence the runtime measurement is very important too. Tab. 1 shows the duration, in seconds, of each filtering method (last column).

6. FUZZY SETS EVALUATION

So, we meet with situation of a hard choice, when one alternative is better in some ways, the other alternative is better in other ways, and neither is better than the other overall.

One of the most popular and efficient approaches in case of reasoning and decision making in presence of uncertainty is based on fuzzy sets theory [9, 10].

In conventional dual logic a statement can be true or false and nothing in between. Most

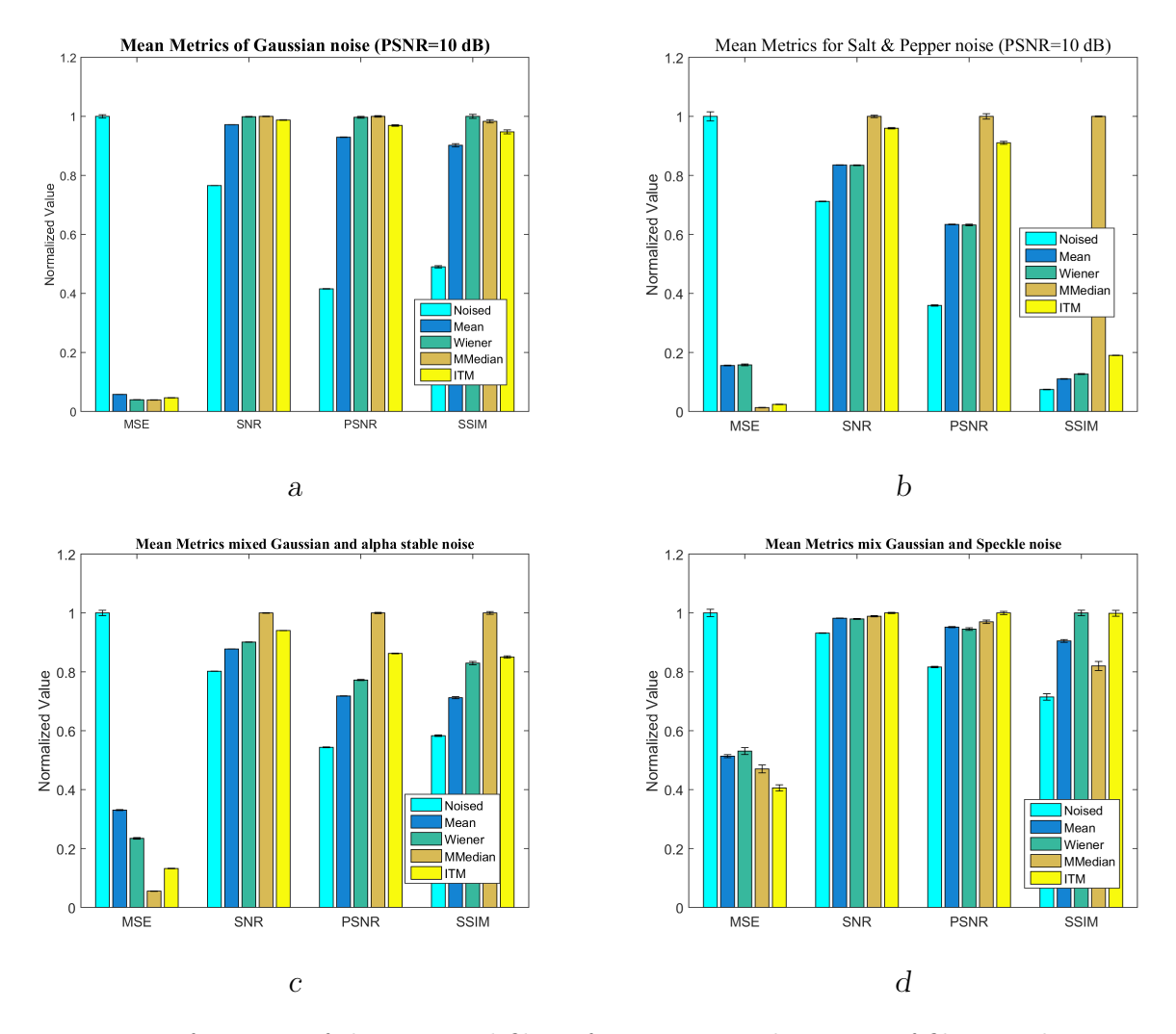


Fig. 4. Performance of the proposed filters for various combinations of filters and noises

of traditional tools for modeling and reasoning are crisp and precise in character. By crisp we mean dichotomous that is, yes-or-no type rather than more-or-less type. However, more often than not the problems in real world are not always true-or false type. Very often real situations are uncertain or vague in a number of ways. From the inception of the theory, a fuzzy set has been defined as a collection of objects with membership values between 0 and 1 (complete exclusion and complete membership). The membership values express the degrees to which each object is compatible with the properties distinctive to the collection.

In case of our study, the class of objects is the "filter class" where each object is one of the four estimated filters: Mean filter, Wiener filter, MMWF filter and ITM filter. For each measure of quality, a fuzzy set is defined, composed by a class of filters (objects) able to suppress the certain noise. In our case, we have four different fuzzy sets, one for each kind of measure: MSE, PSNR and ISSIM. For each fuzzy set, a membership function is defined that, on a scale between 0 and 1 assigns to each filter a grade of membership to the considered fuzzy set. The membership function was constructed in the following way: for each denoising evaluation the minimum and the maximum of every measures was considered, then the filter

Filter	Gauss	Impulse	Gauss+Impulse	Speckle+Gauss	Time (s)
Mean	0.81	0.13	0.62	0.97	7
Wiener	0.99	0.17	0.35	0.92	8
MMWF	0.96	1.00	1.00	0.93	485
ITM	0.90	0.43	0.87	1.00	53

Tab. 2. Fuzzy set evaluation of the best filter for different noises

Tab. 3. Fuzzy set evaluation of the best global filter

Filter		Time (s)		
	without time	without time	all parameters	, ,
		and speckle noise		
Mean	0	0	0	7
Wiener	0	0	0	8
MMWF	0.05	0.83	0	485
ITM	0.34	0.34	0.34	53

performances were rescaled in the range between 0 and 1.

Our goal is to define which filter offers the best performance for contemporaneous denoising of the four different kinds of noise: Gauss noise, impulse noise, Mixture of Gauss and Impulse noise, mixture of speckle and Gauss noise. According to the rules of fuzzy set theory, the best filter is the filter that offers the highest minimum grade of membership between the considered fuzzy sets.

Tab. 2 summarizes the results of the fuzzy sets evaluation of the best filter (all cells contain the membership values and last column contains the time of working of the algorithm). But from the table is still difficult to appreciate which filter gives the best result.

Applying the same approach for this data we can define which filter is best for global denoising.

The "global denoising" set is an intersection of the four different kinds of denoising sets (Impulse noise, Gaussian, Gaussian+Impulse and Gaussian+Speckle) and of the time of computing for every filtering algorithm. For this kind of denoising (Tab. 3, last column), the best filter is the ITM algorithm.

In the context of real experiment sometime we may know that image definitely does not contain some kind of noise or some parameters. Then we cannot consider these factors in our fuzzy set algorithm. For example, the case when time of computing is does not matter and image does not contain speckle noise is presented in column three of the Tab. 3. As it can be seen, in this situation the best filter is the MMWF filter.

7. CONCLUSIONS

The objective of the present study was to show the usefulness of the 3D adaptive spatial filters with advantages that include low cost, easy visualization, and amenability to experimental manipulations.

We compared the performance of the designed 3D MMWF and ITM nonlinear adaptive spatial filters, and of three well-established denoising techniques (Mean, Median, Wiener), for removal of four different kinds of noise: Gaussian (PSNR 10 dB), mix of alpha-stable and Gaussian noise (PSNR 10 dB), mix of speckle and Gaussian noise (PSNR 10 dB) and "salt&pepper" noise.

Extensive computer simulations of the indicates superior results in terms of both quantitative evaluation measuring indices and visual appearance for ITM and MMWF approaches for each of the noise category (impulse or Gaussian) and for contemporary suppression of the different kinds of noise (global denoising). The quantitative evaluations for global denoising were made by means fuzzy sets theory.

Designed filters meet most of the PA image denoising requirements in real practice:

- The proposed filtering approach allows efficient noise suppression, simultaneously preserving unaltered edges and morphology.
- MMWF and ITM filters need only one intuitive clear parameter for tuning.
- Our filters are easy to implement and fast to use.
- The ITM filter uses only arithmetic operations, so it is faster, than filtering based on another principles.
- Developed filters are almost invariant to noise features and do not need a priori information.
- MMWF and ITM filters may be use to non-stationary signals with unstructured variations in intensity and size.

The adaptive characteristics of the MMWF and ITM filters allow consider them as versatile and invariant approaches to reduction of different types of noise, attaining the first score in global denoising.

ЛІТЕРАТУРА

- [1] Li C., Wang L. V. Photoacoustic tomography and sensing in biomedicine // Physics in Medicine and Biology. 2009. Vol. 54, no. 19. P. 59–97.
- [2] Numerical approaches for quantitative analysis of two-dimensional maps: A review of commercial software and home-made systems / Marengo E., Robotti E., Antonucci F., and Cecconi D. // PROTEOMICS. 2005. Vol. 5, no. 3. P. 654–666.
- [3] Mandelbrot B. The Pareto—Lévy law and the distribution of income // International Economic Review. 1960. Vol. 1, no. 2. P. 79–106.

- [4] Janicki A., Weron A. Simulation and chaotic behavior of alpha-stable stochastic processes. Boca Raton, FL: CRC Press, 1993. 376 p.
- [5] Forouzanfar M., Abrishami-Moghaddam H. Principles of waveform diversity and design. Section B Part V: Remote sensing / ed. by Wicks M., Mokole E., Blunt S. et al. SciTech Publishing, 2010. P. 558–577.
- [6] Cannistraci C. V., Montevecchi F. M., Alessio M. Median-modified Wiener filter provides efficient denoising, preserving spot edge and morphology in 2-DE image processing // PROTEOMICS. 2009. Vol. 9, no. 21. P. 4908–4919.
- [7] Xudong J. Iterative truncated arithmetic mean filter and its properties // IEEE Transactions on Image Processing. 2012. Vol. 21, no. 4. P. 1537–1547.
- [8] Image Qualifty Assessment: From Error Visibility to Structural Similarity / Wang Z., Bovik A. C., Sheikh H. R., Hamid R., and Simoncelli E. P. // IEEE Transactions on Image Processing. 2004. Apr. Vol. 13, no. 4. P. 600–612.
- [9] Zadeh L. A. Fuzzy sets // Information and Control. 1965. Vol. 8. P. 338–353.
- [10] Zadeh L. A. Toward a generalized theory of uncertainty // Information Sciences. 2005. Vol. 172. P. 1–40.

REFERENCES

- [1] C. Li and L. V. Wang, "Photoacoustic tomography and sensing in biomedicine," *Physics in Medicine and Biology*, vol. 54, no. 19, pp. 59–97, 2009.
- [2] E. Marengo, E. Robotti, F. Antonucci, and D. Cecconi, "Numerical approaches for quantitative analysis of two-dimensional maps: A review of commercial software and home-made systems," *PROTEOMICS*, vol. 5, no. 3, pp. 654–666, 2005.
- [3] B. Mandelbrot, "The Pareto—Lévy law and the distribution of income," *International Economic Review*, vol. 1, no. 2, pp. 79–106, 1960.
- [4] A. Janicki and A. Weron, Simulation and chaotic behavior of alpha-stable stochastic processes. Boca Raton, FL: CRC Press, 1993.
- [5] M. Forouzanfar and H. Abrishami-Moghaddam, *Principles of waveform diversity and design. Section B Part V: Remote sensing*, ch. Ultrasound speckle reduction in the complex wavelet domain, pp. 558–577. SciTech Publishing, 2010.
- [6] C. V. Cannistraci, F. M. Montevecchi, and M. Alessio, "Median-modified Wiener filter provides efficient denoising, preserving spot edge and morphology in 2-DE image processing," *PROTEOMICS*, vol. 9, no. 21, pp. 4908–4919, 2009.
- [7] J. Xudong, "Iterative truncated arithmetic mean filter and its properties," *IEEE Transactions on Image Processing*, vol. 21, no. 4, pp. 1537–1547, 2012.

- [8] Z. Wang, A. C. Bovik, H. R. Sheikh, R. Hamid, and E. P. Simoncelli, "Image qualifty assessment: From error visibility to structural similarity," *IEEE Transactions on Image Processing*, vol. 13, p. 600–612, Apr. 2004.
- [9] L. A. Zadeh, "Fuzzy sets," Information and Control, vol. 8, pp. 338–353, 1965.
- [10] L. A. Zadeh, "Toward a generalized theory of uncertainty," *Information Sciences*, vol. 172, pp. 1–40, 2005.

О. Г. Рудницький, М. О. Рудницька, Л. В. Ткаченко Попередня обробка й покращення якості зображення при томографічній оптоакустичній реконструкції

Фотоакустичний метод забезпечує чудову оптичну контрастність у поєднанні з глибоким ультразвуковим проникненням і роздільною здатністю для структурної та функціональної медичної візуалізації. У цій роботі ми зосередились на проектуванні тривимірного фільтра для ефективного та всебічного придушення різних видів шумів, які можуть співіснувати в фотоакустичних сигналах. Розглядались просторові фільтри, які мають лише один параметр для налаштування — розмір вікна. Для того, щоб запропонувати найкращий для практичного використання підхід, тривимірні нелінійні адаптивні просторові фільтри — медіанно-модифікований фільтр Вінера (MMWF) та ітераційний усічений арифметичний середній фільтр (ITM) — порівнювали з усталеними методами шумозахисту (середніми, медіанними та вінерівськими фільтрами). Їхню продуктивність було перевірено за допомогою фантома Шеппа–Логана розміром $256 \times 256 \times 256$ вокселів. На додаток до візуальної якості, досліджувались такі параметри як співвідношення сигнал/шум (SNR), середня квадратична похибка (MSE), співвідношення пік/шум (PSNR), структурний індекс подібності (SSIM). Продуктивність запропонованих фільтрів оцінювалась і з точки зору часу, витраченого на обробку. Результати моделювання показали, що ITM і MMWF фільтри перевершують існуючі фільтри, забезпечуючи кращу візуальну якість, PSNR, SSIM і значення MSE для фантома Шеппа–Логана, пошкодженого гаусовим чи імпульсним шумом і сумішшю цих шумів.

КЛЮЧОВІ СЛОВА: шумоізоляція, обробка зображень, фільтр шумозаглушення, просторова фільтрація, фотоакустична візуалізація, нечіткі множини

А. Г. Рудницкий, М. А. Рудницкая, Л. В. Ткаченко Предварительная обработка и улучшение качества изображения при томографической оптоакустической реконструкции

Фотоакустический метод обеспечивает превосходный оптический контраст в сочетании с глубоким ультразвуковым проникновением и разрешением для структурной и функциональной медицинской визуализации. В этой работе мы сконцентрировались на разработке трехмерного фильтра для эффективного и всестороннего подавления шумов различного типа, могущих сосуществовать в фотоакустических сигналах. Рассматривались пространственные фильтры, которые имеют только один параметр для настройки — размер окна. Для того, чтобы

предложить лучший для практического использования подход, нелинейные трехмерные адаптивные пространственные фильтры — модифицированный по медиане фильтр Винера (ММWF) и итеративный усеченный арифметический средний фильтр (ITM) — сравнивали с хорошо известными методами шумоподавления (средними, срединными и винеровскими фильтрами). Их работоспособность была проверена с помощью фантома Шеппа—Логана размером 256 × 256 × 256 вокселей. В дополнение к визуальному качеству, исследовались такие параметры как отношение сигнал/шум (SNR), среднеквадратичная ошибка (МSE), пиковое отношение сигнал/шум (PSNR) и структурный индекс подобия (SSIM). Производительность предлагаемых фильтров оценивалась и с точки зрения времени, затраченного на обработку. Результаты моделирования показали, что фильтры ITM и MMWF превосходят существующие подходы, обеспечивая лучшие визуальное качество и значения PSNR, SSIM, МSE для фантома Шеппа—Логана, искаженного гауссовским или импульсным шумом и смесью этих шумов.

КЛЮЧЕВЫЕ СЛОВА: шумоизоляция, обработка изображений, фильтр шумоподавления, пространственная фильтрация, фотоакустическая визуализация, нечеткие множества